Matrix analysis of microring coupled-resonator optical waveguides

Joyce K. S. Poon, Jacob Scheuer, Shayan Mookherjea, George T. Paloczi, Yanyi Huang, and Amnon Yariv

Department of Electrical Engineering and Department of Applied Physics, California Institute of Technology, MS 136-93, Pasadena, CA 91125

poon@caltech.edu

www.its.caltech.edu/∼poon

Abstract: We use the coupling matrix formalism to investigate continuous-wave and pulse propagation through microring coupled-resonator optical waveguides (CROWs). The dispersion relation agrees with that derived using the tight-binding model in the limit of weak inter-resonator coupling. We obtain an analytical expression for pulse propagation through a semi-infinite CROW in the case of weak coupling which fully accounts for the nonlinear dispersive characteristics. We also show that intensity of a pulse in a CROW is enhanced by a factor inversely proportional to the inter-resonator coupling. In finite CROWs, anomalous dispersions allows for a pulse to propagate with a negative group velocity such that the output pulse appears to emerge before the input as in "superluminal" propagation. The matrix formalism is a powerful approach for microring CROWs since it can be applied to structures and geometries for which analyses with the commonly used tight-binding approach are not applicable.

OCIS codes: (230.5750) Resonators; (230.7370) Waveguides; (230.3120) Integrated optics devices

References and links

1. A. Yariv, Y. Xu, R. K. Lee, and A. Scherer, "Coupled-resonator optical waveguide: a proposal and analysis," Opt. Lett. **24**, 711–713 (1999).
2. Y. Xu, R. K. Lee, and A. Yariv, "Propagation and second-harmonic generation of electromagnetic waves in a coupled-resonator optical waveguide," J. Opt. Soc. Am. B **77**, 387–400 (2000).
3. N. Stefanou and A. Modinos, "Impurity bands in photonic insulators," Phys. Rev. B **57**, 12 127–12 133 (1998).
4. D. N. Christodoulides and N. K. Efremidis, "Discrete temporal solitons along a chain of nonlinear coupled microcavities embedded in photonic crystals," Opt. Lett. **27**, 568–570 (2002).
5. S. Mookherjea and A. Yariv, "Kerr-stabilized super-resonant modes in coupled-resonator optical waveguides," Phys. Rev. E **66**, 046 610 (2002).
6. J. E. Heebner and R. W. Boyd, "'Slow' and 'fast' light in resonator-coupled waveguides," J. Mod. Opt. **49**, 2629–2636 (2002).
7. C. K. Madsen, "General IIR optical filter design for WDM applications using all-pass filters," IEEE J. Lightwave Technol. **18**, 860–868 (2000).
8. G. Lenz, B. J. Eggleton, C. K. Madsen, and R. E. Slusher, "Optical delay lines based on optical filters," IEEE J. Quantum Electron. **37**, 525–532 (2001).
9. B. E. Little, S. T. Chu, W. Pan, D. Ripin, T. Kaneko, Y. Kokubun, and E. Ippen, "Vertically coupled glass microring resonator channel dropping filters," IEEE Photon. Technol. Lett. **11**, 215–217 (1999).
10. M. Bayindir, B. Temelkuran, and E. Ozbay, "Tight-binding description of the coupled defect modes in three-dimensional photonic crystals," Phys. Rev. Lett. **84**, 2140–2143 (2000).
11. A. Yariv and P. Yeh, *Optical waves in crystals: Propagation and control of laser radiation* (Wiley, New York, 1984).

#3181 - $15.00 US Received 14 October 2003; revised 19 December 2003; accepted 22 December 2003

12. K. Oda, N. Takato, and H. Toba, "A wide-FSR waveguide double-ring resonator for optical FDM transmission systems," IEEE J. of Lightwave Technol. **9**, 728–736 (1991).
13. R. Orta, P. Savi, R. Tascone, and D. Trinchero, "Synthesis of multiple-ring resonator filters for optical systems," IEEE Photon. Technol. Lett. **7**, 1447–1449 (1995).
14. J. V. Hryniewicz, P. P. Absil, B. E. Little, R. A. Wilson, and P.-T. Ho, "Higher order filter response in coupled microring resonators," IEEE Photon. Technol. Lett. **12**, 320–322 (2000).
15. A. Melloni, R. Costa, P. Monguzzi, and M. Martinelli, "Ring-resonator filters in silicon oxynitride technology for dense wavelength-division multiplexing systems," Opt. Lett. **28**, 1567–1569 (2003).
16. A. Yariv, "Universal relations for coupling of optical power between microresonators and dielectric waveguides," Electron. Lett. **36**, 321–322 (2000).
17. B. E. Little, S. T. Chu, H. A. Haus, J. Foresi, and J.-P. Laine, "Microring resonator channel dropping filter," IEEE J. Lightwave Technol. **15**, 998–1005 (1997).
18. A. Melloni and F. Morichetti, "Linear and nonlinear pulse propagation in coupled resonator slow-wave optical structures," Opt. Quantum Electron. **35**, 365–379 (2003).
19. J. E. Heeber, R. W. Boyd, and Q.-H. Park, "SCISSOR solitons and other novel propagation effects in microresonator-modified waveguides," J. Opt. Soc. Am. B **19**, 722–731 (2002).
20. S. Mookherjea and A. Yariv, "Pulse propagation in a coupled-resonator optical waveguide to all orders of dispersion," Phys. Rev. E **65**, 056 601 (2002).
21. A. D. Poularikas, *The handbook af formulas and tables for signal processing* (IEEE Press, New York, 1998).
22. G. T. Paloczi, Y. Huang, A. Yariv, and S. Mookherjea, "Polymeric Mach-Zehnder interferometer using serially coupled microresonators," Opt. Express **11**, 2666–2671 (2003).
23. S. Longhi, M. Marano, M. Belmonte, and P. Laporta, "Superluminal pulse propagation in linear and nonlinear photonic grating structures," IEEE. J. Sel. Top. Quantum Electron. **9**, 4–16 (2003).
24. M. Bayindir, S. Tanriseven, and E. Ozbay, "Propagation of light through localized coupled-cavity modes in one-dimensional photonic band-gap structures," Appl. Phys. A **72**, 117–119 (2001).
25. W. Chen and D. L. Mills, "Gap solitons and the nonlinear optical-response of superlattices," Phys. Rev. Lett. **58**, 160–163 (1987).
26. C. M. de Sterke and J. E. Sipe, "Envelope-function approach for the electrodynamics of nonlinear periodic structures," Phys. Rev. A **38**, 5149–5165 (1988).
27. C. M. de Sterke, D. G. Salinas, and J. E. Sipe, "Coupled-mode theory for light propagation through deep nonlinear gratings," Phys. Rev. E **54**, 1969–1989 (1996).
28. B. J. Eggleton, R. E. Slusher, C. M. de Sterke, P. A. Krug, and J. E. Sipe, "Bragg grating solitons," Phys. Rev. Lett. **76**, 1627–1630 (1996).
29. D. N. Christodoulides and R. I. Joseph, "Slow Bragg solitons in nonlinear periodic structures," Phys. Rev. Lett. **62**, 1746–1749 (1989).
30. Little Optics press release, "Higher order optical filters using microring resonators" (Little Optics, 2003), http://www.littleoptics.com/hofilter.pdf.

1. Introduction

Coupled optical resonators are becoming important in nonlinear optics research as well as in telecommunication applications [1, 2, 3, 4, 5, 6]. Systems consisting of a few coupled resonators, say $1 < N < 5$, have been proposed for optical filtering and modulation [7, 8, 9]. On the other extreme, "large" systems, say $N > 10$, can be regarded as a new type of waveguide termed Coupled-Resonator Optical Waveguide (CROW) with unique and controllable dispersion properties [3, 1, 2, 10].

The "large" chains (CROWs) have been previously analyzed using a tight-binding formalism [1]. In the tight-binding method, we approximate the electric field of an eigenmode $\mathbf{E}_K$ of the CROW as a Bloch wave superposition of the individual resonator modes $\mathbf{E}_\Omega$ [1],

$$\mathbf{E}_K(\mathbf{r},t) = E_0 \exp(i\omega_K t) \sum_n \exp(-inK\Lambda)\mathbf{E}_\Omega(\mathbf{r} - n\Lambda\hat{\mathbf{z}}), \tag{1}$$

where the nth resonator in the chain is centered at $z = n\Lambda$. Under the assumption of symmetric nearest neighbor coupling, the dispersion relation of the CROW is [1]

$$\omega_K = \Omega\left[1 - \frac{\Delta\alpha}{2} + \kappa_1 \cos(K\Lambda)\right], \tag{2}$$

#3181 - $15.00 US Received 14 October 2003; revised 19 December 2003; accepted 22 December 2003

where Ω is the resonant frequency of an individual resonator and $\Delta\alpha$ and κ_1 are defined as

$$\Delta\alpha = \int \mathrm{d}^3\mathbf{r}[\varepsilon(\mathbf{r}) - \varepsilon_0(\mathbf{r})]\mathbf{E}_\Omega(\mathbf{r}) \cdot \mathbf{E}_\Omega(\mathbf{r}) \tag{3a}$$

$$\kappa_1 = \int \mathrm{d}^3\mathbf{r}[\varepsilon_0(\mathbf{r} - \Lambda\hat{\mathbf{z}}) - \varepsilon(\mathbf{r} - \Lambda\hat{\mathbf{z}})] \times \mathbf{E}_\Omega(\mathbf{r}) \cdot \mathbf{E}_\Omega(\mathbf{r} - \Lambda\hat{\mathbf{z}}). \tag{3b}$$

$\varepsilon(\mathbf{r})$ is the dielectric coefficient of the CROW and $\varepsilon_0(\mathbf{r})$ is the dielectric coefficient of an individual resonator. Therefore, the coupling parameter κ_1 represents the overlap of the modes of two neighboring resonators and $\Delta\alpha/2$ gives the fractional self frequency shift of ω_K.

Even though much of the theoretical work on CROWs is based on the tight-binding method [2, 5], the formalism is not convenient for practical, physical systems. For example, it does not account for input/output coupling, loss, different resonator sizes, or variations in coupling strengths. With the aim of rigorously analyzing realistic CROW structures, we use a matrix approach [11, 12, 13] to study a system consisting of N coupled ring resonators with input and output waveguides. Since the modal properties of ring resonators can be easily tailored and their fabrication technology is mature [14, 15], they may enable practical implementations of CROWs.

2. Transfer matrix formalism

We first consider an infinite chain of coupled ring resonators in order to obtain its dispersion relation. Both forward and backward propagating waves exist in an individual resonator, as shown in Fig. 1. We assume the coupling region is sufficiently long compared to λ, so that

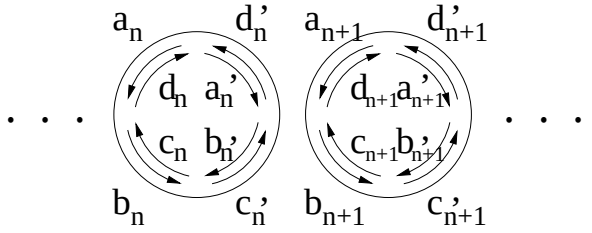

Fig. 1. An infinitely long chain of coupled ring resonators, with the forward and backward propagating field components labelled.

the light circulating in one direction in a resonator is phase-matched to only one of the two degenerate counter-propagating modes of the adjacent resonator. Using the notation of Fig. 1, the coupling between two adjacent rings can thus be described by [16]

$$\begin{bmatrix} b'_n \\ b_{n+1} \end{bmatrix} = \begin{bmatrix} t & \kappa \\ -\kappa^* & t^* \end{bmatrix} \begin{bmatrix} a'_n \\ a_{n+1} \end{bmatrix}, \qquad \begin{bmatrix} d'_n \\ d_{n+1} \end{bmatrix} = \begin{bmatrix} t & \kappa \\ -\kappa^* & t^* \end{bmatrix} \begin{bmatrix} c'_n \\ c_{n+1} \end{bmatrix} \tag{4}$$

where t and κ are respectively the dimensionless transmission and coupling coefficients over the coupling length. The matrix is unitary and unimodular so that $|t|^2 + |\kappa|^2 = 1$. Defining a vector with the different field components,

$$x_n = \begin{bmatrix} a \\ b \\ c \\ d \end{bmatrix}_n, \tag{5}$$

#3181 - $15.00 US Received 14 October 2003; revised 19 December 2003; accepted 22 December 2003

Equation (4) can be rewritten as

$$x_{n+1} = \begin{bmatrix} P & 0 \\ 0 & P \end{bmatrix} x'_n \equiv \mathbb{P} x'_n \tag{6a}$$

$$P = \frac{1}{\kappa} \begin{bmatrix} -t & 1 \\ -1 & t^* \end{bmatrix} \tag{6b}$$

As the field propagates around the ring, it accumulates a phase shift and may be attenuated, so

$$x'_n = \begin{bmatrix} 0 & Q \\ Q & 0 \end{bmatrix} x_n \equiv \mathbb{Q} x_n \tag{7a}$$

$$Q = \begin{bmatrix} 0 & \mathrm{e}^{-i\beta R\pi} \\ \mathrm{e}^{i\beta R\pi} & 0 \end{bmatrix} \tag{7b}$$

In the above definition, R is the ring radius and $\beta = n(\omega)\omega/c + i\alpha$, where $n(\omega)$ is the frequency dependent effective index and α is the loss (or gain) per unit length in the ring. Combining (6) and (7), we have

$$x_{n+1} = \mathbb{P}\mathbb{Q} x_n \tag{8}$$

Equation (8) is completely general. The matrices $\mathbb{P}$ and $\mathbb{Q}$ can be specified at each frequency to account for any frequency dependence of the effective index, loss, and transmission and coupling coefficients.

3. CROW dispersion relation

From a theoretical point of view, it is important to understand how the tight-binding and matrix approaches are related to each other. We shall show the matrix method embodied in Eq. (8) converges to the tight-binding result in Eq. (2) under certain approximations. The approach we adopt is similar to the transfer matrix analysis of a Bragg stack [11].

The field in one resonator of the CROW as specified by x_n is

$$\mathscr{E}(\rho,\phi) = \mathbf{E}(\rho) \times \begin{cases} a_n \exp[i\beta R(\pi-\phi)] + d_n \exp[-i\beta R(\pi-\phi)] & 0 < \phi < \pi \\ b_n \exp[-i\beta R(\pi+\phi)] + c_n \exp[i\beta R(\pi+\phi)] & -\pi < \phi < 0 \end{cases} \tag{9}$$

where ϕ is the azimuthal angle relative to the propagation direction in the counter-clockwise sense, and ρ is the radial co-ordinate. For a mode of an infinite chain of ring resonators, the fields are periodic at the lattice constant, Λ. So applying Bloch's theorem,

$$x_{n+1} = \exp(-iK\Lambda) x_n, \tag{10}$$

where K is the CROW propagation constant. Combining this requirement with (8) leads to

$$\mathrm{Det}|\mathbb{P}\mathbb{Q} - \exp(-iK\Lambda)U| = \mathrm{Det}|(PQ)^2 - \exp(-i2K\Lambda)U| = 0, \tag{11}$$

where U is the identity matrix.

We assume lossless propagation and $\mathrm{Im}(\kappa) \gg \mathrm{Re}(\kappa)$ for phase-matched coupling. We recall that at the resonant frequency of an individual resonator, Ω, $\Omega n(\Omega)R/c = m$, where m is an integer, and $n(\Omega)$ is the effective index at Ω. Therefore, approximating $n(\Omega) \approx n(\omega_K)$, we solve Eq. (11) to obtain

$$\sin(\frac{\omega_K}{\Omega} m\pi) = \pm \mathrm{Im}(\kappa) \cos(K\Lambda), \tag{12}$$

which is the desired dispersion relation for a ring CROW. This relation is exact in the sense that it involves no assumption about the coupling strength.

#3181 - $15.00 US Received 14 October 2003; revised 19 December 2003; accepted 22 December 2003

If we expand Eq. (12) in the parameter $\Delta\omega m\pi/\Omega$, $\Delta\omega \equiv \omega_K - \Omega$, we obtain to first order

$$\frac{\omega_K}{\Omega} = 1 \pm \kappa_2 \cos(K\Lambda), \tag{13}$$

where $\kappa_2 \equiv \mathrm{Im}(\kappa)/(m\pi)$. The two dispersion relations corresponding to the '$\pm$' coexist for an infinite structure to allow for both forward and backward wave propagation (i.e. positive and negative group velocities). Physically, for a finite structure without reflection and a uni-directional input as in Fig. 3, only the dispersion relation with the matching group and phase velocities as the input wave will be of significance.

Equation (13) is of a form identical to the tight-binding result in Eq. (2). The correction $\Delta\alpha/2$ term does not explicitly appear in Eq. (13) since it is accounted for by $\mathrm{Re}(\kappa)$. From Eq. (13), it follows that for $\Delta\omega m\pi/\Omega \ll 1$, it is necessary that $|\kappa| \ll 1$. This condition and the absence of all but the nearest neighbor coupling are thus the validity conditions for the tight-binding approximate result (13).

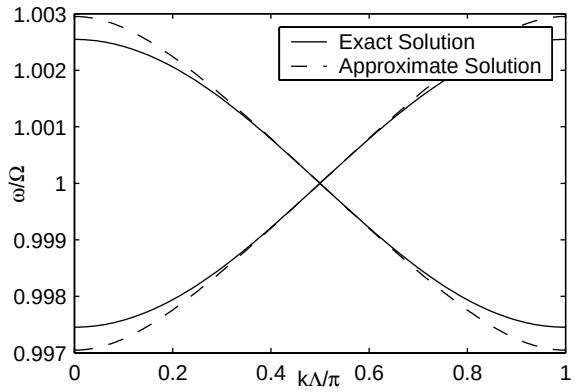

Fig. 2. The exact and cosine-approximate (i.e. tight-binding-approximate) dispersion relations for $m = 100$ and $\kappa = -0.8i$.

Figure 2 shows the dispersion relations for $\kappa = -0.8i$ and $m = 100$ as calculated using the "exact" form in Eq. (12) and the approximated form in Eq. (13). As ω_K/Ω increases, the exact dispersion relation deviates more significantly from the cosine form. For smaller values of κ, the deviation from the cosine dispersion relation is reduced.

The Bloch modes of the CROW are given by the eigenvectors of $\mathbb{PQ}$. At each frequency, there are 4 Bloch modes corresponding to the 4 eigenvalues (i.e. values of K). The eigenvalues are $\exp(-iK_1\Lambda) \equiv \xi_1$, $\exp[-i(K_1\Lambda+\pi)] \equiv -\xi_1$, $\exp(-iK_2\Lambda) \equiv \xi_2$, and $\exp[-i(K_2\Lambda+\pi)] \equiv -\xi_2$. The corresponding (un-normalized) eigenvectors are

$$\hat{q}_{\xi_1} = \begin{bmatrix} \zeta+\gamma \\ 1 \\ \zeta+\gamma \\ 1 \end{bmatrix}, \quad \hat{q}_{-\xi_1} = \begin{bmatrix} -(\zeta+\gamma) \\ -1 \\ \zeta+\gamma \\ 1 \end{bmatrix}, \quad \hat{q}_{\xi_2} = \begin{bmatrix} \zeta-\gamma \\ 1 \\ \zeta-\gamma \\ 1 \end{bmatrix}, \quad \hat{q}_{-\xi_2} = \begin{bmatrix} -(\zeta-\gamma) \\ -1 \\ \zeta-\gamma \\ 1 \end{bmatrix}, \tag{14}$$

where

$$\gamma = \frac{1}{2t}\sqrt{1+\exp(\frac{-4im\pi\omega}{\Omega})+2\exp(\frac{-2im\pi\omega}{\Omega})(1-2t^2)}, \tag{15a}$$

$$\zeta = \frac{1}{2t}\left[1+\exp(\frac{2im\pi\omega}{\Omega})\right]. \tag{15b}$$

#3181 - $15.00 US Received 14 October 2003; revised 19 December 2003; accepted 22 December 2003

The 4 eigenvectors are orthogonal to each other and they represent standing waves in each resonator. In the limit of weak coupling $|\kappa| \ll 1$ and $\omega \approx \Omega$, such that $\gamma \approx |\kappa| \approx 0$, $\zeta \approx 1$, and $\xi_1 = \xi_2$, the 4 eigenvectors reduce to 2 degenerate eigenvectors, representing the two different superpositions of the clockwise and counter-clockwise propagating waves in a single resonator:

$$\hat{q}_{\xi_1} = \hat{q}_{\xi_2} = \begin{bmatrix} 1 \\ 1 \\ 1 \\ 1 \end{bmatrix}, \quad \hat{q}_{-\xi_1} = \hat{q}_{-\xi_2} = \begin{bmatrix} -1 \\ -1 \\ 1 \\ 1 \end{bmatrix}. \tag{16}$$

In the limit of strong coupling and $\omega \approx \Omega, t \ll 1$, $\gamma + \zeta \approx \sqrt{\frac{1+|\kappa|}{1-|\kappa|}} \approx \frac{2}{t}$, and $\zeta - \gamma \approx \sqrt{\frac{1-|\kappa|}{1+|\kappa|}} \approx 0$. The eigenvectors become

$$\hat{q}_{\xi_1} = \begin{bmatrix} \frac{2}{t} \\ 1 \\ \frac{2}{t} \\ 1 \end{bmatrix}, \quad \hat{q}_{-\xi_1} = \begin{bmatrix} -\frac{2}{t} \\ -1 \\ \frac{2}{t} \\ 1 \end{bmatrix}, \quad \hat{q}_{\xi_2} = \begin{bmatrix} 0 \\ 1 \\ 0 \\ 1 \end{bmatrix}, \quad \hat{q}_{-\xi_2} = \begin{bmatrix} 0 \\ -1 \\ 0 \\ 1 \end{bmatrix}. \tag{17}$$

We observe that 2 field components are significantly stronger than the other. This corresponds to a wave that "zig-zags" through the resonators without making complete round-trips in each resonator. The asymptotic behavior of the eigenvectors confirms the physical picture that as $|\kappa| \to 0$, the modes of the CROW are essentially the modes of the independent resonators, and as $|\kappa| \to 1$, the microrings no longer act as resonators and the CROW modes are essentially conventional waveguide modes.

4. Finite CROWs and a travelling wave picture

For physical realizations of CROWs, we are interested in finite structures with input and output coupling. These properties cannot be readily dealt with using the tight-binding method, but can be easily incorporated into the transfer matrices. Figure 3 shows a typical implementation of a microring CROW: light is coupled into and out of a set of coupled ring resonators via the input and output waveguides. Assuming that the coupling length between waveguides and the CROW is long compared to λ, then only the travelling wave phase-matched to the input can be excited.

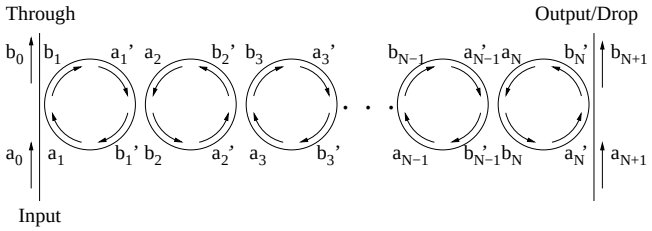

Fig. 3. A CROW consisting of N ring resonators with input and output waveguides.

Adopting the notation in Fig. 3, the fields between adjacent resonators are related by

$$\begin{bmatrix} a \\ b \end{bmatrix}_{n+1} = PQ \begin{bmatrix} a \\ b \end{bmatrix}_n, \tag{18}$$

#3181 - $15.00 US Received 14 October 2003; revised 19 December 2003; accepted 22 December 2003

where P and Q are defined in Eq. (6) and Eq. (7).

By cascading the transfer matrices, PQ, we obtain an expression for the field components at the output of the CROW after N identical rings:

$$\begin{bmatrix} a_{N+1} \\ b_{N+1} \end{bmatrix} = P_{out} Q (PQ)^{N-1} P_{in} \begin{bmatrix} a_0 \\ b_0 \end{bmatrix} \equiv \begin{bmatrix} A & B \\ C & D \end{bmatrix} \begin{bmatrix} a_0 \\ b_0 \end{bmatrix}, \tag{19}$$

where P_{in} and P_{out} describe the coupling between the CROW and the input/output waveguides. For a single input to the waveguide, we set $a_{N+1} = 0$. Therefore, the transfer functions at the "through" and "output" ports as shown in Fig. 3 are

$$\frac{b_0}{a_0} = -\frac{A}{B} \equiv T_{thr}(\omega), \tag{20a}$$

$$\frac{b_{N+1}}{a_0} = C - \frac{AD}{B} \equiv T_{out}(\omega). \tag{20b}$$

As in microring filter design [17], the coupling between the waveguides and the CROW can be selected to maximize the flatness of the transmission response. Therefore, a finite CROW can be designed to mimic an infinite CROW over a bandwidth with a sufficiently flat transmission response.

An advantage of the matrix formalism is that it is valid for chains of any length N, which is essential in analyzing any physical realization of a CROW. From the phase response of the transmission function given by Eq. (20), we can deduce the dispersion relation of the structure. However, we note that the travelling wave is not an eigenmode of the CROW, since the Bloch modes as given by the eigenvectors of $\mathbb{PQ}$ are standing waves as in Eq. (14). A travelling wave solution is formed by a superposition, either the sum or difference, of the two Bloch modes with equal group velocities (i.e. $\hat{q}_{\xi_1}$ and $\hat{q}_{-\xi_1}$, or $\hat{q}_{\xi_2}$ and $\hat{q}_{-\xi_2}$). The travelling wave is an eigenvector of $(PQ)^2$, and it is verified that the sense of propagation in the rings alternates between clockwise and counter-clockwise with each operation of $\mathbb{PQ}$, as depicted in Fig. 3. Therefore, taking the phase difference accumulated over two rings to be $-2K\Lambda$, where K is the Bloch wave vector, such that the phase difference between the output and the input is approximately $-(N-1)K\Lambda$, we can determine the CROW dispersion from the finite structure.

As an example, we compute the dispersion relation of a finite CROW consisting of 20 coupled rings with inter-resonator and waveguide-resonator coupling constants of $-0.5i$. The rings are lossless, and their radius is 16.4μm. n_{eff} is taken to be constant and equal to 1.5. Figure 4 compares the dispersion relation extrapolated from the finite CROW with the dispersion relation of an infinite CROW as given by Eq. (12). The small amplitude ripples are manifested at the resonance frequencies of the finite structure. In the limit of an infinite number of resonators, the resonance peaks will be infinitesimally close to each other and the ripples will be smoothed out.

5. Pulse propagation

Pulse propagation through CROWs are of particular technological interest, since information transmitted in optical communication systems is typically encoded in pulses. Using the results from the previous sections, we can analytically and numerically study optical pulse propagation in semi-infinite and finite microring CROWs.

5.1. Semi-infinite case

A semi-infinite microring CROW consists of an infinitely long CROW coupled to a single input waveguide as in Fig. (5). The input waveguide ensures that only a pulse of positive (or negative)

#3181 - $15.00 US Received 14 October 2003; revised 19 December 2003; accepted 22 December 2003

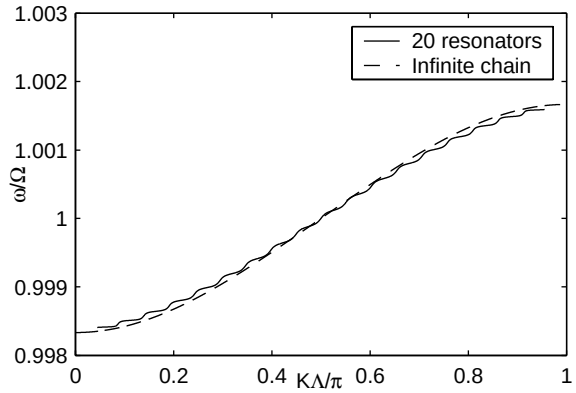

Fig. 4. The exact dispersion relation for an infinite CROW and the dispersion relation as extracted from 20 coupled resonators. The rings have a radius of 16.4μm and the inter-resonator coupling is $-0.5i$.

group velocity propagates through the structure. Assuming that the bandwidth of the input pulse is within the bandwidth of the CROW band such that all of the input light is coupled into the waveguide, the field amplitude b_1 in the first resonator is $b_1(\omega) = -1/\kappa_{in} a_0(\omega)$, where κ_{in} is the coupling coefficient between the input waveguide and the first resonator. Since $|\kappa_{in}| < 1$, the intensity of the field inside the CROW is higher than that of the input pulse by $1/|\kappa_{in}|^2$. This does not violate energy conservation, as the increased intensity is a consequence of the reduced group velocity and hence the spatial compression of the pulse inside the CROW. Using the dispersion relation in Eq. (13), the maximum group velocity in the CROW is

$$v_{g,\max} = \frac{|\kappa|\Lambda\Omega}{m\pi}. \tag{21}$$

Defining the "slowing" factor as in Ref. [18] to be

$$S = \frac{c}{n_{\text{eff}} v_{g,\max}}, \tag{22}$$

and approximating $\Lambda \simeq 2R$, S can be expressed as

$$S = \frac{\pi}{2|\kappa|}. \tag{23}$$

Therefore, for $\kappa_{in} = \kappa$, the intensity inside the rings is roughly enhanced by $(\frac{2}{3}S)^2$. This result makes intuitive sense since the only loss mechanism for the otherwise lossless resonators is the inter-resonator coupling. Interestingly, even though the energy velocity of the Bloch modes at Ω corresponds to the group velocity $v_{g,\max}$[11], the energy velocity of a wave that is fully coupled into the semi-infinite CROW is proportional to $|\kappa|^2$. Hence, the intensity enhancement is proportional to the energy velocity reduction rather than the group velocity reduction.

Also, in contrast to CROWs, for other coupled resonator structures where there is no feedback between the resonators, such as the SCISSOR [19], the slowing factor is approximately proportional to $1/|\kappa|^2$ in the case of weak coupling. However, a CROW has the advantage that, even in the presence of loss, it is most transmitting for the frequencies of the CROW band, while a side-coupled resonator is most attenuating near the resonant frequency of the resonator.

To analyze the temporal dynamics a pulse launched into the semi-infinite CROW, we adopt a method of analysis that is analogous to pulse propagation in conventional waveguides such

#3181 - $15.00 US Received 14 October 2003; revised 19 December 2003; accepted 22 December 2003

as optical fibers. We shall find in the limit of weak coupling, such that Eq. (13) is a good approximation, there exists a closed-form solution to the evolution of any arbitrary input pulse.

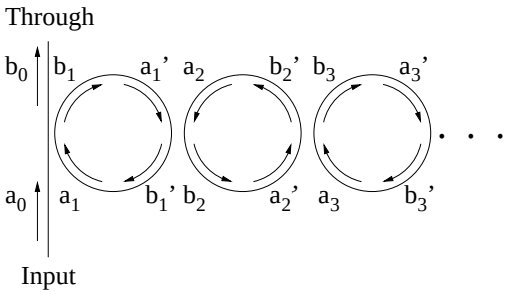

Fig. 5. A semi-infinite CROW.

The electric field at where b_1 is taken, $\mathscr{E}(t,z=0)$, can be expressed as the Fourier integral

$$\mathscr{E}(t,z=0)=\int_{band}\mathrm{d}\omega b_1(\omega)\exp(i\omega t), \tag{24a}$$

$$b_1(\omega)=\int\frac{\mathrm{d}t'}{2\pi}\mathscr{E}(t',z=0)\exp(-i\omega t'). \tag{24b}$$

At $z=N\Lambda$, each frequency component, $b_1(\omega)$, acquires a phase shift of $NK\Lambda$, so the field is

$$\mathscr{E}(t,z=N\Lambda)=\int_{band}\mathrm{d}\omega\exp(i\omega t)\int\frac{\mathrm{d}t'}{2\pi}\mathscr{E}(t',z=0)\exp[-i(\omega t'+K(\omega)N\Lambda)]. \tag{25}$$

However, $K(\omega)$ is given by the dispersion relation of the CROW, Eq. (13). Therefore, instead of integrating over frequency in (25), if we integrate over the half of the Brillouin zone that gives the appropriate group velocity (for example, the right half), we obtain

$$\begin{aligned}\mathscr{E}(t,z=N\Lambda)= \quad & -\Lambda\Omega\kappa_2 e^{i\Omega t}\textstyle\int_0^{\pi/\Lambda}\mathrm{d}K\sin(K\Lambda)e^{-iKN\Lambda}e^{i\Omega\kappa_2\cos(K\Lambda)(t-t')} \\ & \textstyle\int\frac{\mathrm{d}t'}{2\pi}\mathscr{E}(t',z=0)e^{-i\Omega t'}.\end{aligned} \tag{26}$$

Equation (26) can be further simplified by letting $x=K\Lambda$, and invoking the Jacobi-Anger expansion [20],

$$e^{i\Omega\kappa\cos(x)(t-t')}=\sum_m c_m J_m[\Omega\kappa_2(t-t')]\cos(mx) \tag{27a}$$

$$c_m=\begin{cases}1 & \text{if } m=0\\ 2i^m & \text{if } m>0\end{cases}, \tag{27b}$$

to arrive at

$$\begin{aligned}\mathscr{E}(t,z=N\Lambda)= \quad & -\Omega\kappa_2 e^{i\Omega t}\textstyle\sum_m c_m\int_0^{\pi}\mathrm{d}x\sin(x)\cos(mx)e^{-ixN} \\ & \textstyle\int\frac{\mathrm{d}t'}{2\pi}J_m[\Omega\kappa_2(t-t')]\mathscr{E}(t',z=0)e^{-i\Omega t'}.\end{aligned} \tag{28}$$

However, $\alpha_{m,N}=\int_0^{\pi}\mathrm{d}x\sin(x)\cos(mx)e^{-ixN}\neq 0$ only for certain values of m and N:

$$\alpha_{m,N}=\begin{cases}\frac{i\pi}{4} & \text{for } N=m-1 \text{ and } N=-m-1\\ -\frac{i\pi}{4} & \text{for } N=m+1 \text{ and } N=-m+1\\ \frac{-2(m^2+N^2-1)}{(m^2+N^2-1)^2-4m^2N^2} & \text{for } N+m=\text{even}\end{cases} \tag{29}$$

#3181 - $15.00 US Received 14 October 2003; revised 19 December 2003; accepted 22 December 2003

So the equation for the pulse envelope $E(t,z)$, such that $\mathscr{E}(t,z) = E(t,z)e^{i\Omega t}$, is given by the convolution integral

$$E(t, z = N\Lambda) = -\frac{\kappa_2 \Omega}{2\pi} \sum_m c_m \alpha_{m,N} \int \mathrm{d}t' J_m[\Omega\kappa_2(t-t')] E(t', z=0). \tag{30}$$

The Fourier transform of a Bessel function $J_n(t)$ is only defined within $|2\pi f| \leq 1$ [21], which accounts for the finite bandwidth of the CROW, $\Omega(1-|\kappa_2|) \leq \omega \leq \Omega(1+|\kappa_2|)$.

Equation (30) holds for an arbitrary input pulse and its sole assumption is the cosine-approximate dispersion relation, which is valid for small κ. The nonlinear dispersive nature of the CROW is embodied in the summation over the Bessel functions. Figure 6(a) shows the evolution of a Gaussian input pulse $E(t,z=0) = \exp(-t^2/T^2)$ as calculated using Eq. (30). Figure 6(b) shows the numerical results obtained from the transfer matrices. The analytical solution is in excellent agreement with the fully numerical approach. As the pulse propagates, even though the main peak travels at the group velocity, the ripples develop only at the tail end of the pulse.

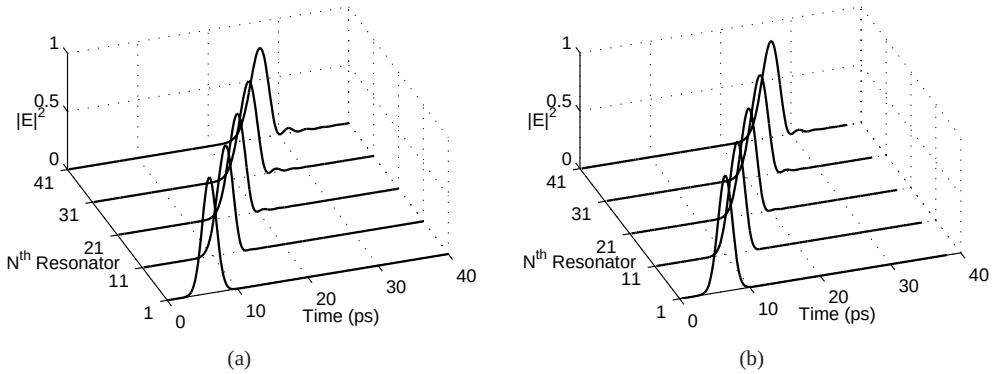

Fig. 6. Evolution of a 2.4ps (FWHM) Gaussian pulse centered about 1.5μm in a semi-infinite CROW with $\kappa_2 = 0.0016$. The fields are normalized to the maximum field amplitude in the first resonator. (a) Theoretical results computed using Eq. (30). (b) Results computed numerically with the transfer matrices using a chain of 100 ring resonators ($n_{\mathrm{eff}} = 1.5$, $R = 16\mu$m).

5.2. Finite case

Pulse propagation through finite CROWs can be easily analyzed using the transfer matrices results of Eq. (20). Since Eq. (20) is specified at each frequency, we simply have to find the product between the transfer functions and the spectral components of the input pulse. The temporal behavior follows naturally from the Fourier transform.

Distortionless propagation through an arbitrary finite CROW can always be achieved if the input pulse is sufficiently narrow-band such that the transmission function of the drop port, as defined in Fig. 3, over the pulse bandwidth is near unity. However, short pulses which become distorted as they propagate in the CROW are also of fundamental interest. For this purpose, we take an example consisting of 10 coupled ring resonators of radius 164.5μm and $n_{\mathrm{eff}} = 1.5$. The inter-resonator coupling constant is $-0.3i$ and the coupling between the waveguides and CROW is $-0.5i$. The transfer characteristics of this structure are shown in Fig. (7). We launch a 30.5ps (FWHM) long pulse centered at 1.55μm into the CROW.

#3181 - $15.00 US Received 14 October 2003; revised 19 December 2003; accepted 22 December 2003

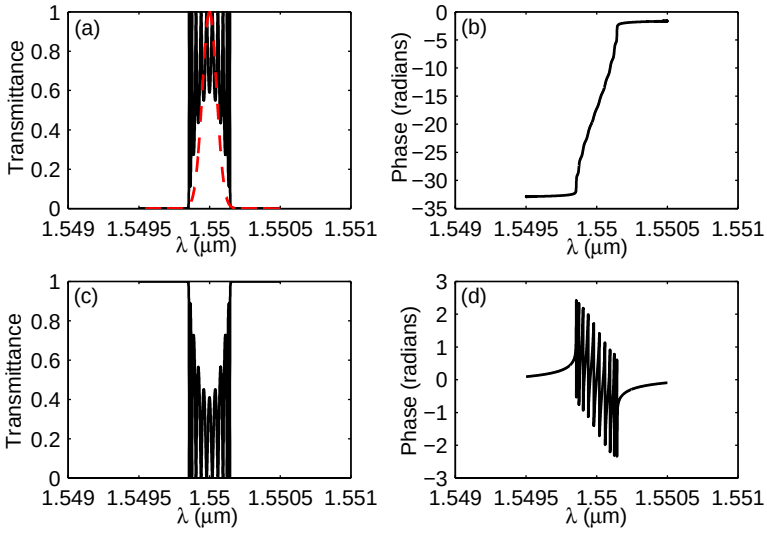

Fig. 7. The transmission characteristics of a 10 ring long CROW. The ring radius is 164.5μm and $n_{\text{eff}} = 1.5$. Inter-resonator coupling is $-0.3i$ and the waveguide-CROW coupling is $-0.5i$. A 30.5 ps (FWHM) long pulse centered at 1.55μm is input into the CROW. (a) Transmittance of at the drop port. The dashed line shows the spectrum of the input pulse. (b) Phase response at the drop port. (c) Transmittance at the through port. (d) Phase response at the through port.

Using the transfer matrices, we can examine how a pulse evolves in the CROW by finding the transfer functions associated with a_n or b_n. Figure 8 shows the evolution of the pulse through the CROW. Even though the output pulse is attenuated compared to the input, the field intensity inside the rings can be greater than the input, as in the case of the semi-infinite CROW. The intensity build-up is verified by a FDTD simulation discussed in Sect. 5.3. The significant increase in the intensity of the input pulse inside the CROW can be used to enhance the strengths of nonlinear optical interactions. As noted earlier, we can account for loss (or gain) in our model by including an imaginary part to the propagation factor β. We have found the transfer matrices give excellent agreement with experimental results [22].

Another interesting effect is the small amplitude ripple that follows the main peak in each resonator. The ripple is travelling from the end of the CROW back to the start at approximately the group velocity of the forward moving pulse. This is analogous to a reflection from the end of a waveguide, though in the microring CROW described here there are no reflection mechanisms as the coupling is assumed to be perfectly phase-matched. Indeed, Fig. 9 shows that the ripple at the through port is delayed from the the drop port pulse by the travelling time between the input and the drop. Therefore, although the microring CROW is composed of "microscopic," discrete elements, it possesses certain "macroscopic" properties that mimic conventional waveguides.

At the through port, we may obtain negative group velocities, which some researchers refer to as "superluminal propagation." [23, 6] In the time domain, the main (highest) peak of the output pulse does indeed appear before the peak of the input pulse. Figure 9 shows the output pulses at the through and drop ports as well as in the input pulse. The peak of the through pulse is approximately 5ps before than the peak of the input, as though the output appears before the input. However, the pulse is attenuated and distorted. This behavior is accounted for by the anomalous dispersive properties at the through port in Fig. 7(d). The anomalous dispersion is

#3181 - $15.00 US Received 14 October 2003; revised 19 December 2003; accepted 22 December 2003

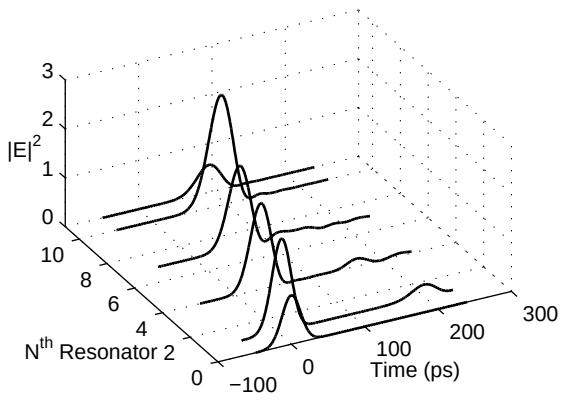

Fig. 8. The pulse transmission through the CROW described in Fig. (7). The $0th$ resonator is the input pulse and the $11th$ resonator is the output pulse at the drop port.

also confirmed by the FDTD simulation discussed in the next section.

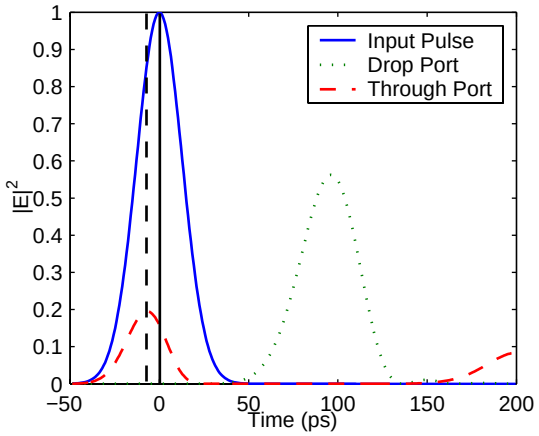

Fig. 9. The input pulse and the output pulses at the drop and through ports of the the CROW described in Fig. (7). The solid vertical line marks the maximum of the input pulse, and the dashed vertical line marks the maximum of the output pulse at the through port. The peak of the through port pulse occurs about 5ps sooner than the peak of the input.

5.3. FDTD simulations

As a test for the transfer matrix method and a confirmation of the intensity build-up and anomalous dispersion, we use a finite difference time domain (FDTD) simulation to study the pulse propagation through two coupled ring resonators. The waveguides and rings are 0.2μm wide. They are set in air and have an index of refraction of 3.5. The rings have a radius of 5μm, and the wavelength dependent effective index, as extrapolated from a separate FDTD simulation of the waveguides, is $n_{\text{eff}} = 3.617 - 0.5539\lambda$. The coupling between the rings is $-0.32i$, and the coupling between the rings and the waveguides is $-0.4i$. A 2.4ps (FWHM) Gaussian pulse is launched into the system, and the fields at the through port, drop port, and inside the rings are monitored. We compare the transfer matrix method with the FDTD simulation in Fig. 10(a), showing that the approaches are in excellent agreement. The anomalous dispersion at

#3181 - $15.00 US Received 14 October 2003; revised 19 December 2003; accepted 22 December 2003

the through port and the increase in intensity in the coupled rings are confirmed by the FDTD simulation and are evident in Fig. 10(b).

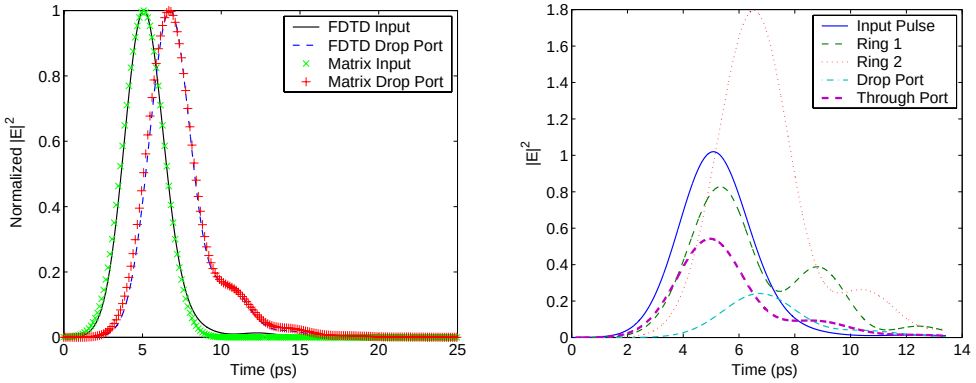

(a) (b)

Fig. 10. FDTD simulation of 2 coupled ring resonators with input and output waveguides. The radius of the rings is 5μm, and the effective index is $n_{\text{eff}} = 3.617 - 0.5539\lambda$. The inter-resonator coupling is $-0.32i$ and the waveguide-resonator coupling is $-0.4i$. The input pulse is a 2.4ps (FWHM) Gaussian centered at 1.55μm. (a) Comparison between the FDTD simulation and the transfer matrix method. Output refers to the drop port. (b) Intensity built-up and anomalous dispersion as confirmed by the FDTD simulation.

6. Comparison with Fabry-Perot resonators

The transfer matrix analysis discussed here is general and can be applied to Bragg stacks and Fabry-Perot resonators as well. A Bragg stack can be regarded as a chain of coupled Fabry-Perot etalons. Bayindir *et al.* have recently demonstrated a CROW operating near 600nm using coupled Fabry-Perot resonators fabricated in a multi-layer fashion [24]. There have also been extensive studies in the linear and nonlinear optical propagation in Bragg stacks [11, 25, 26, 27, 28, 29]. In Fabry-Perot resonators, the coupling parameter κ corresponds to the transmission coefficient, while t corresponds to the reflection coefficient. They can be calculated from the Fresnel coefficients or from an analysis of a Bragg stack in the case of a Fabry-Perot with Bragg end mirrors [11]. The two major differences between the Fabry-Perot resonator and the ring resonator are 1) the former can be fully described by a 2×2 transfer matrix while the latter requires a 4×4 matrix, and 2) the reflection and transmission coefficients may contain a real part. Therefore, in contrast to the $\pm\cos(K\Lambda)$ dependence in Eq. (13), there is only one dispersion curve for a Fabry-Perot CROW at a given frequency range and there may also be an additional phase shift in the cosine dependence.

In contrast to ring resonators, the coupling between Fabry-Perot resonators with Bragg end mirrors is controlled by Bragg reflection. Even though the coupling coefficient may be more stringently controlled in these structures, ring resonators remain an attractive option for CROWs in planar integrated optical circuits because they can be fabricated in a single lithographic step. Moreover, recent developments in coupled ring resonators in polymer and semiconductor materials illustrate the potential of using ring resonators as constituent elements in CROWs [22, 30].

#3181 - $15.00 US Received 14 October 2003; revised 19 December 2003; accepted 22 December 2003

7. Conclusion

In summary, the transfer matrix method is used to analyze microring coupled resonators. The transfer matrix and tight-binding approaches yield equivalent dispersion relations in the limit of weak coupling. We also study pulse propagation through semi-infinite and finite CROWs to find intensity enhancement as well as anomalous dispersion. The matrix method can account for finite chains, holds for any coupling strength, applies to travelling waves, and can treat heterogeneous chains consisting of an arbitrary mix of resonators and coupling constants. These features make the transfer matrices versatile for device design and for analyzing experimental results of microring CROWs [22].

Acknowledgments

The authors thank Dr. Y. Xu, J. Choi, W. Green, and W. Liang for helpful discussions. J. Poon acknowledges support from the Natural Sciences and Research Council of Canada. The support of DARPA, the Office of Naval Research, and the Air Force Office of Scientific Research are gratefully acknowledged.

#3181 - $15.00 US Received 14 October 2003; revised 19 December 2003; accepted 22 December 2003